



Direct conversion of biomass components to the biofuel methyl levulinate catalyzed by acid-base bifunctional zirconia-zeolites

Hu Li^{a,b,c}, Zhen Fang^{a,c,*}, Jia Luo^c, Song Yang^b

^a Biomass Group, College of Engineering, Nanjing Agricultural University, 40 Dianjiangtai Road, Nanjing, Jiangsu 210031, China

^b State-Local Joint Engineering Laboratory for Comprehensive Utilization of Biomass, Center for R&D of Fine Chemicals, Guizhou University, Guiyang 550025, China

^c Chinese Academy of Sciences, Biomass Group, Key Laboratory of Tropical Plant Resources and Sustainable Use, Xishuangbanna Tropical Botanical Garden, 88 Xuefulu, Kunming, Yunnan 650223, China

ARTICLE INFO

Article history:

Received 10 April 2016

Received in revised form 5 July 2016

Accepted 6 July 2016

Available online 7 July 2016

Keywords:

Biomass

Biofuels

Acid-base bifunctionality

Methyl levulinate

Microwave

ABSTRACT

A series of metal-zeolite hybrids was prepared by impregnation and deposition-precipitation methods and characterized with different techniques. Catalytic performance of these catalysts on microwave-assisted conversion of selected carbohydrates to the fuel component methyl levulinate (ML) in methanol was studied. It was demonstrated that metal oxide content/type and acid-base bifunctionality were closely correlated with substrate conversion and ML yield, respectively. Among various as-prepared catalysts, zirconia-zeolite hybrid ZrY6(0.5) with moderate acid-base site content (0.97 & 0.08 mmol g⁻¹), high stability and porosity (average mesopore diameter: 6.2 nm) exhibited superior catalytic activity. At 180 °C, around 67–73%, 78%, 53% and 27% yields of ML could be achieved from monosaccharides (e.g., glucose, mannose and galactose), sucrose, starch and cellulose, respectively. The Zr-Y6(0.5) hybrid exhibited good stability, and could be reused for five times with ML yields of ≥63% from glucose.

© 2016 Elsevier B.V. All rights reserved.

1. Introduction

Excessive consumption of fossil resources (e.g., petroleum and coal) that are not renewable has been causing serious problems such as environmental pollution and global warming. In this respect, a steady shift to utilize renewable materials for producing high-value organic compounds and biofuels are being made through environment-friendly processes [1,2]. Levulinic acid (LA), one of the twelve important biomass-derived chemicals released by the U.S. Department of Energy (DOE) [3], is recognized as a promising platform molecule to produce biochemicals such as plasticisers, resins, herbicides, flavouring agents and solvents, as well as biofuels [4–7]. For producing LA from glucose-based sugars, high temperatures (around 200 °C) were typically involved in the presence of mineral acids (e.g., HCl and H₂SO₄) [8]. In view of the recyclable and easy to handle nature, heterogeneous catalysts are preferable [9–12]; however, only a limited number of solid acids such as SO₃H-

functionalized materials and sulfate/phosphate metal oxides are efficient for this reaction [13–17].

Polymerization and potential cross-polymerization were reported to significantly reduce process selectivity to LA from carbohydrates [18]. In a hydrothermal process, insoluble (49.6% yield) and water-soluble humins (5.5% yield) at complete cellulose conversion were detected at 220 °C [19]. In strong contrast, microwave-assisted catalytic system could selectively transform cellulose into LA with good yields of ~60% over homogeneous acids such as acidic ionic liquids, HCl and SnCl₄ at 160–200 °C in 0.5–2 h [20–24]. As compared with conventional heating, microwave irradiation appears to exhibit relatively higher selectivity in transformation of biopolymers to LA [25].

The platform molecule LA can be further upgraded to alkyl levulimates (ALs) such as methyl- and ethyl levulimates (ML & EL) through esterification with various alcohols, which are deemed as 'second generation' biofuels [26]. Starting from purified LA, methyl to butyl levulimates could be produced in good yields (35–99%) over acidic catalysts such as heteropolyacids, H₂SO₄, sulphated oxides, and Amberlyst-15 [27]. Without separating LA from the reaction mixture, direct conversion of carbohydrates to ALs was more attractive despite their yields are relatively low (<50%) from substrates containing glucose units in most cases [27]. Solid catalysts with high molar ratios of Brønsted acid to Lewis acid could enhance the

* Corresponding author at: Biomass Group, College of Engineering, Nanjing Agricultural University, 40 Dianjiangtai Road, Nanjing, Jiangsu 210031, China.

E-mail addresses: huli_0414@126.com (H. Li), zhenfang@njau.edu.cn, zhen.fang@mail.mcgill.ca (Z. Fang), luojia@xtbg.ac.cn (J. Luo), jhxz.msm@gmail.com (S. Yang).

URL: <http://biomass-group.njau.edu.cn/> (Z. Fang).

formation of ALs by preventing the generation of by-products in alcohols [28–31], while ethyl glucoside other than EL was selectively attained from glucose in ethanol catalyzed by a sole Brønsted acid such as sulfonated SBA-15 materials and SO₃H-functionalized ionic liquids [32,33]. Therefore, the appropriate control of active sites in solid functional catalysts is crucial to improve the selectivity of downstream valuable products derived from biomass derivatives containing glucose units.

In our previous studies, both hydrolysis and dehydration processes have been demonstrated to be accelerated by microwave irradiation [34–37]. Under traditional hydrothermal conditions, zeolites exhibited extensive uses in selective conversion of biomass derivatives to specific chemicals [38]; however, production of alkyl levulinates from sugars with zeolites in high catalytic efficiency is rarely reported. Recently, Si-OH groups and metal oxides in zeolite frameworks were illustrated to be capable of absorbing microwave, and a significantly enhanced interaction of microwaves was detected in water [39]. In the present work, a series of metal-zeolite hybrids was prepared from metal salts and zeolites by impregnation or deposition-precipitation method, and their structures were studied by different characterization techniques. These porous solid hybrids with both acid and base sites were screened for direct and efficient production of methyl levulinate (ML) from various sugars under microwave irradiation.

2. Materials and methods

2.1. Materials

FeCl₃·6H₂O (99.0%), CuCl₂·3H₂O (99.0%), ZrOCl₂·8H₂O (98.0%), ZnCl₂ (\geq 98.0%), and ammonium hydroxide (AR, 25–28%) were supplied by Shanghai Aladdin Industrial Incorporation. Methanol (98.0%), glucose (99.5%), mannose (99.0%), galactose (98.0%), fructose (\geq 99.0%), sucrose (99.5%), cellobiose (98.0%), starch, cellulose (microcrystalline, powder), ML (99.0%), methyl lactate (MLA, 98.0%), and HMF (99.0%) were bought from Shanghai Sigma-Aldrich. HY2.6, NH₄-Y6 and NH₄-Y30 (with a Si/Al molar ratio of 2.6, 6 & 30, respectively), NH₄-β19 (Si/Al molar ratio: 19), and NH₄-ZSM-5 (Si/Al molar ratio: 15) were purchased from the Zeolyst International (US). Other Reagents (AR) were used as obtained, only when they are otherwise mentioned.

2.2. Preparation of metal-zeolite hybrids

The proton form of zeolites (HY, H β , and HZSM-5) were initially prepared from zeolites in ammonium form by calcination at 550 °C (heating rate: 5 °C min⁻¹) in air for 6 h in a tubular furnace. Two different methods (i.e., impregnation and deposition-precipitation) were subsequently adopted for the preparation of metal-zeolite hybrids [hereafter denoted as metal-zeolite(x), x(metal/zeolite, mmol/g)=0.25, 0.5, 1, and 2] by using activated zeolites as acidic solid supports and different metal salts (i.e., FeCl₃·6H₂O, CuCl₂·3H₂O, ZnCl₂, and ZrOCl₂·8H₂O) with different molar loadings relative to the weight of zeolite as the metal precursors. For samples prepared by impregnation (denoted as IP), zeolite (1.0 g) was first added into an aqueous solution of metal salt (0.25–2.0 mmol, 25 mL) and stirred at 500 rpm at room temperature for 3 h. The obtained slurry after filtration (0.45 μm pore size) was dried overnight at 120 °C, followed by calcination in air at 450 °C for 6 h (heating rate: 2 °C min⁻¹).

Deposition-precipitation catalysts (denoted as DP) were prepared by mixing zeolite (1.0 g) with an aqueous solution containing a certain weight of metal salts (0.25–1.0 mmol, 25 mL) at a fixed pH of 9–10, which was controlled by NH₄OH. After aged for 2 h under ambient and stirring (500 rpm) conditions, the slurry was filtered

(0.45 μm pore size), washed with deionized-water until the filtrate was neutral, and dried overnight at 120 °C. The resulting material was calcined with the identical procedure and final temperature as impregnation samples.

For comparison, ZrO₂ was prepared from ZrOCl₂·8H₂O under ambient conditions via a precipitation method at NH₄OH-controlled pH of 9–10. The sample was completely washed with deionized-water, dried at 120 °C for 6 h, and calcined at 450 °C in air for 6 h using the above-mentioned heating process, Mesh sieves (200-mesh) was used to screen out samples in relatively uniform and small sizes for catalytic experiments.

2.3. Catalyst characterization

Thermogravimetry (TG) analysis was conducted using a thermogravimetric analyzer (Netzsch STA 429 instrument, Germany) in the range of 25–800 °C with a heating rate of 10 °C min⁻¹ under N₂ atmosphere (flow rate: 30 mL min⁻¹). Compositions (Si, Al, and Zr) of solid samples were measured by ICP-OES (Optima 5300 DV instrument, PerkinElmer Incorporation, MA) after being dissolved in water by HNO₃ and HF. FT-IR spectra were tested with Nicolet iS 10 FT-IR instrument (KBr disc; ThermoFisher, MA) over the range of 400–4000 cm⁻¹. XRD patterns were recorded with a D/max-TTR III X-ray powder diffractometer (Rigaku International Corporation, Tokyo) using a radiation source of Cu K α . BET surface areas and BJH pore sizes of the samples were obtained from N₂ physisorption measurements (Micromeritics ASAP 2010 instrument, GA). Pyridine-adsorbed FT-IR spectra were recorded with a Bruker VERTEX V70v system. Before pyridine adsorption, the sample prepared as a thin self-supporting wafer was heated to 200 °C (heating rate: 5 °C min⁻¹), and degassed until the residual pressure was below 0.05 Pa. Then pyridine was introduced, followed by degassing and heating at 100 °C to remove physisorbed pyridine. The resulting pyridine-adsorbed sample was subjected to a temperature-programmed desorption at 150, 250, and 350 °C (heating rate: 5 °C min⁻¹) for 30 min, respectively, which was in situ recorded with FT-IR. The surface acidity/basicity of solid catalysts were assessed with NH₃/CO₂-TPD (AutoChem II 2920 chemisorption analyzer, Micromeritics, Georgia), respectively. During TPD analysis, the catalyst (around 100 mg) was initially placed in a quartz reactor and degassed at 300 °C for 60 min (heating rate 5 °C min⁻¹), followed by cooling to 40 °C under He flow (50 mL min⁻¹). For NH₃-TPD, the degassed sample was flushed with 10% NH₃ in 90% He (60 mL min⁻¹) at 40 °C for 90 min to allow the adsorption of NH₃, and then NH₃ desorption was measured by a thermal conductivity detector every one second from 40 to 550 °C with a heating rate of 5 °C min⁻¹ under He flow of 50 mL min⁻¹. The operational conditions of CO₂-TPD are same to those of NH₃-TPD except the ammonia desorption process, wherein the NH₃ desorption was recorded at a maximum temperature of 450 °C (heating rate 5 °C min⁻¹) under He flow of 50 mL min⁻¹ for 1–2.5 h.

2.4. Conversion of sugars to ML

In a typical procedure, a solid catalyst (30 mg) was added into a stock solution (5 mL) of sugar in methanol with a concentration of 10–60 g/L that was prepared before and distributed into a glass vial (10 mL). After stirring for 3–5 min under ambient conditions, the resulting mixture was placed into a well-controlled microwave synthesis reactor (Monowave 300, Anton Paar, Graz, Austria). The reaction solution was heated to a desired temperature (140–180 °C) within 3 min and magnetically stirred at 800 rpm for specific reaction time (excluding initial heating and final cooling times, see Supplementary information for details of the microwave reactor), which was well maintained by a proportional-integral-derivative (PID) controller (Fig. S1). After reaction, solid components were sep-

arated from the product mixture using a centrifuge (3–30 K, SIGMA, Osterode am Harz, Germany) at 18,000 rpm (30,427 relative centrifugal force) for 2 min, and the liquid sample was filtered with a 0.45 µm syringe filter for further analyses. For polysaccharides (i.e., starch and cellulose) and extra amount of glucose insoluble into methanol, the concentration denotes the weight of biomass relative to methanol volume. Selected experiments were repeated 2–3 times with standard deviation (σ) of 0.6–3.2% for ML yield, and 0.5–2.8% for sugar conversion.

2.5. Recycle of catalyst

Solid samples recovered by centrifugal separation were washed with acetone for 1–2 times and dried at 60 °C for 2 h [93–95% catalyst mass recovery efficiency, defined as (weight of recovered catalyst)/(weight of fresh catalyst) × 100%], and were directly used for recycling experiments. The recovery of methanol can be easily fulfilled by distillation since most of the generated products, intermediates, and polymer by-products with higher boiling points (~200 °C) than that of methanol (64.7 °C). Although dimethyl ether (ME) may also be formed in the reaction system, it has a much lower boiling point (−23 °C) than methanol, which renders this by-product to be highly volatile even at room temperature.

2.6. Product analysis

ML, HMF and intermediates in methylated form [e.g., 5-methoxymethylfurfural (MMF), methyl lactate (MLA), ME, methyl glucoside (MG) and methyl fructoside (MF)] in methanol were identified with Gas Chromatography (GC; Agilent 6890N, CA)–Mass Spectrometry (MS; Agilent 5973, CA). Sugar concentrations (e.g., fructose, glucose, mannose, galactose, sucrose, and cellobiose) and furanic compounds in methanol phase (dilution with H₂O for 10 times) were quantified by HPLC (LC-20A, Shimadzu) equipped with a refractive index detector and an Aminex HPX-87H column (Bio-Rad, CA). Representative GC–MS and HPLC spectra of the reaction mixture being conducted at 180 °C for 60 min are shown in Fig. S2. With a more rapid method, glucose in methanol was primarily measured with a highly sensitive Biological Sensor (SBA-40X, Shandong Academy of Sciences, China) by referring to the concentration of glucose standard, and selected results were cross-checked with HPLC. Whereas, ML and MLA were analyzed on GC (GC-2014, Shimadzu, Kyoto) with a Rtx-Wax capillary column (30 m × Ø0.25 mm × 0.25 µm) and a flame ionization detector. Naphthalene was used as internal standard for quantification of ML and MLA. The relative response factors of the standard samples to impurity were in the range of 0.96–1.05 (Fig. S3), and the calibration curves prepared by internal or external standard method are provided in Fig. S4. The yields of the intermediates including MG and MMF, observed in HPLC but not commercial available, were estimated quantitatively by using glucose and HMF as a standard to calibrate, respectively. The conversion of sugars (X, mol%) and ML yield (Y, mol%) were determined and calculated with below equations according to the standard curves of commercial samples ($R^2 \geq 0.998$).

$$X(\%) = [1 - (\text{mole concentration of sugar in product} / (\text{mole concentration of initial sugar}))] \times 100\% \quad (1)$$

$$Y(\%) = (\text{mole concentration of ML} / (\text{mole concentration of initial monosaccharide units})) \times 100\% \quad (2)$$

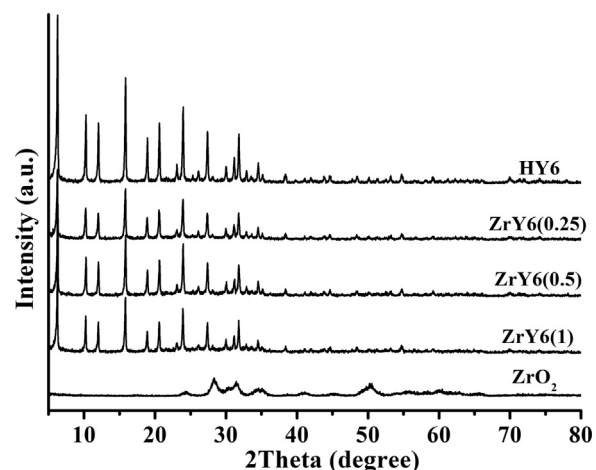


Fig. 1. XRD patterns of ZrO₂, HY6, and ZrY6 hybrids.

3. Results and discussion

3.1. Characterization of catalysts

3.1.1. Crystallinity

Fig. 1 shows XRD patterns of HY6, ZrO₂, and ZrY6 hybrids that are calcined at 450 °C. Neat zirconia is generally amorphous at <400 °C, which is gradually crystallized to generate the tetragonal phase (2θ ≈ 30.5° & 34.6°) if calcined at ≥400 °C. Moreover, two broad peaks around 28.4° and 31.5° were from monoclinic zirconia, and the formation of cubic phase was confirmed by the wide bands at 50.4° and 60.1°. For HY6 zeolite, all peaks were from the FAU (faujasite) structure characterized by intense reflections at 2θ ≈ 6.4°, 23.7° and 15.8° [40]. Owing to zirconia primarily presenting in non-crystalline phase, no distinguishable characteristic reflection of zirconia was observed in ZrY6 hybrids prepared by DP method. Moreover, good dispersion of Zr species and limited segregation of the oxide particles were likely to obscure zirconia from being detected with XRD, implying dimensions of ZrO₂ below the instrumental detection limit of around 2 nm [41]. Moreover, the particle diameters of HY zeolite and these hybrid samples calculated from the Scherrer Equation were almost in the same size (0.48–0.50 µm) [42].

3.1.2. Infrared spectroscopy

The structures of ZrO₂, HY6, and ZrY6 hybrids were analyzed by FT-IR in the range of 400–4000 cm^{−1} (Fig. 2). All samples exhibited absorptions at around 3450 and 1630 cm^{−1}, due to the stretching vibrations of the water molecule –OH groups and the bending vibration of water molecules, respectively. Absorptions at ~490 and 800 cm^{−1} for ZrO₂ were characteristics of Zr–O bonds. For HY6 and ZrY6 hybrids, the almost constant region of 400–1300 cm^{−1} indicated the intact framework vibration of lattice cell (R–O–R unit; where R is SiO₄ or AlO₄ tetrahedron) [40]. Whereas, no unique indication of zirconia was observed in the case of ZrY6 hybrids, which was probably ascribed to the overlapped bands of zirconia and HY6 zeolite, and the relatively low amount of ZrO₂ that is undetected by the instrument.

3.1.3. Elemental composition

Compositions of HY6 and ZrY hybrid catalysts were further determined by ICP-OES analyses on Si, Al and Zr (Table 1). The ammonium form of Y zeolite with a Si/Al molar ratio of 6 (NH₄-Y6) is commercial available, and Si/Al ratio was measured as 5.32 after calcination at 550 °C for 6 h. All these ZrY6 hybrids prepared by DP method were found to have low silicon content, which was pos-

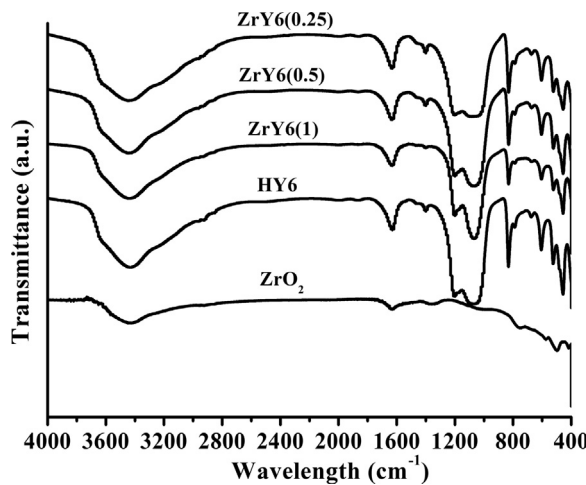


Fig. 2. FT-IR spectra of ZrO_2 , HY6, and ZrY6 hybrids.

sibly contributed to the framework Si atoms selectively extracted by alkali treatment [43]. On the other hand, the increase in zirconia content of the hybrids implied the need of more base, which might play a role in further reducing the molar ratio of Si/Al. Moreover, the actual Zr contents were slightly lower than the controlled contents, due to the loss in the separation and washing steps before drying and calcination.

3.1.4. Surface area and porosity

N_2 adsorption-desorption isotherms were used to evaluate the texture characteristics of ZrO_2 , HY6 and ZrY6 hybrids and BJH pore-size distributions (Fig. 3). It can be observed that the hysteresis loops of isotherms for all samples located in the range of 0.40–0.95 relative pressures (Fig. 3a) strongly indicate the presence of micro-pores and mesopores in the samples, which are consistent with the pore-size distributions shown in Fig. 3b. Table 1 summarizes BET surface areas and average pore diameters of ZrO_2 , HY6 and ZrY6 hybrids. As compared with HY6 and ZrY6 hybrid, ZrO_2 was observed to show a higher average mesopore diameter (ca. 7.4 nm) but lower specific surface area (ca. $94.8 \text{ m}^2 \text{ g}^{-1}$), and intergranular pores were deduced to be primarily resulted from the assembly of ZrO_2 particles. Interestingly, ZrY6 hybrid exhibited superior mesopore diameters (ca. 6.0–6.5 nm) and comparable specific surface areas ($606.0\text{--}655.7 \text{ m}^2 \text{ g}^{-1}$) to HY6 (mesopore diameter: 5.8 nm, and surface area: $702.7 \text{ m}^2 \text{ g}^{-1}$), wherein the alkaline-treated process involving desilication was likely to be responsible for the increase of pore size. Although the mesopore diameter of the ZrY6 hybrid slightly decreased with the rise of zirconia content from 0.25 to 1.0 mmol/g, a critical surface area of $655.7 \text{ m}^2 \text{ g}^{-1}$ was noticed for ZrY6(0.5). It seemed that the zirconia content directly affected the textural properties of the hybrids.

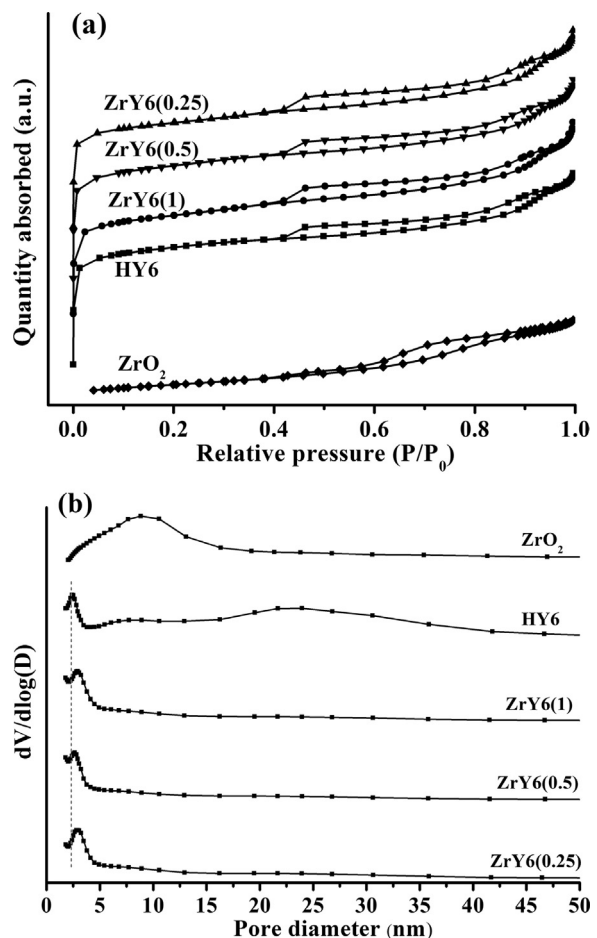


Fig. 3. BET analyses of ZrO_2 , HY6, and ZrY6 hybrids: (a) nitrogen adsorption isotherms and (b) BJH pore-size distributions.

3.1.5. Acidity and basicity

In addition, $\text{NH}_3\text{-TPD}$ was conducted to determine the strength and contents of the acid sites in the catalyst surface of HY6 and ZrY6 hybrid (Fig. 4). It can be observed that Y6 zeolite-based catalysts have two desorption bands located at $\sim 130^\circ\text{C}$ (big) and 400°C (small), corresponding to the weak and medium acid strength, as well as more and less acid site density, respectively. In Table 1, ZrY6(0.5) showed a higher acid site content than the rest, which was possibly attributed to additional weak acid sites in situ formed from zirconia, relatively larger surface area and increased pore size that facilitates the access of NH_3 (Fig. 5). ZrO_2 is a widely studied acid-base bifunctional catalyst [44], and its acid-base site content was determined by NH_3 - and CO_2 -TPD, respectively (Table 1). Given this, the contents of ZrO_2 deposited onto HY6 zeolite would def-

Table 1

Elemental contents, textural properties and acid/base site density of ZrO_2 , HY6 and ZrY6 hybrid catalysts prepared by deposition-precipitation.

Sample	Elemental content		Textural property			Acid/base site density	
	Zr content (mmol/g) ^a		Si/Al molar ratio	BET surface area ($\text{m}^2 \text{ g}^{-1}$)	Pore size (nm)		Acidity (mmol/g)
	Control	Actual			D_{meso} ^b	D_{mean} ^c	
ZrO_2	–	–	–	94.8	7.4	6.78	0.35
HY6	–	–	5.32	702.7	5.8	1.13	0.82
ZrY6(0.25)	0.25	0.24	4.98	606.0	6.5	1.72	0.88
ZrY6(0.5)	0.5	0.45	4.53	655.7	6.2	1.61	0.97
ZrY6(1)	1.0	0.87	4.49	614.6	6.0	1.63	0.79

^a The molar loading of Zr relative to the weight of HY6.

^b Mesopore size (D_{meso}) was obtained from the BJH adsorption average pore diameter.

^c Average pore size (D_{mean}) was estimated by BET (4V/A).

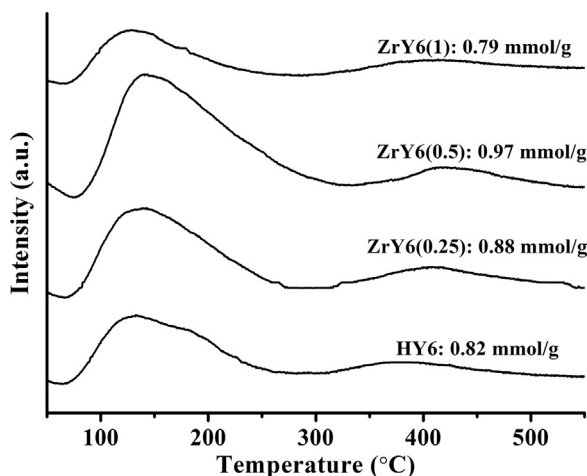


Fig. 4. NH_3 -TPD profiles of HY6 and ZrY6 hybrids.

initely affect the acid/base site density of the resulting hybrids. HY6(0.25) and HY6(0.5) with a relatively low content of zirconia had both increased acid and base site density. In contrast, HY6(1) showed a higher alkali site quantity but a decrease in acid sites. It was proposed that the deposition of more zirconia content might result in the blockage of pore channels, thus hindering the exposure of acid sites inside zeolite pores to NH_3 . Moreover, the introduction

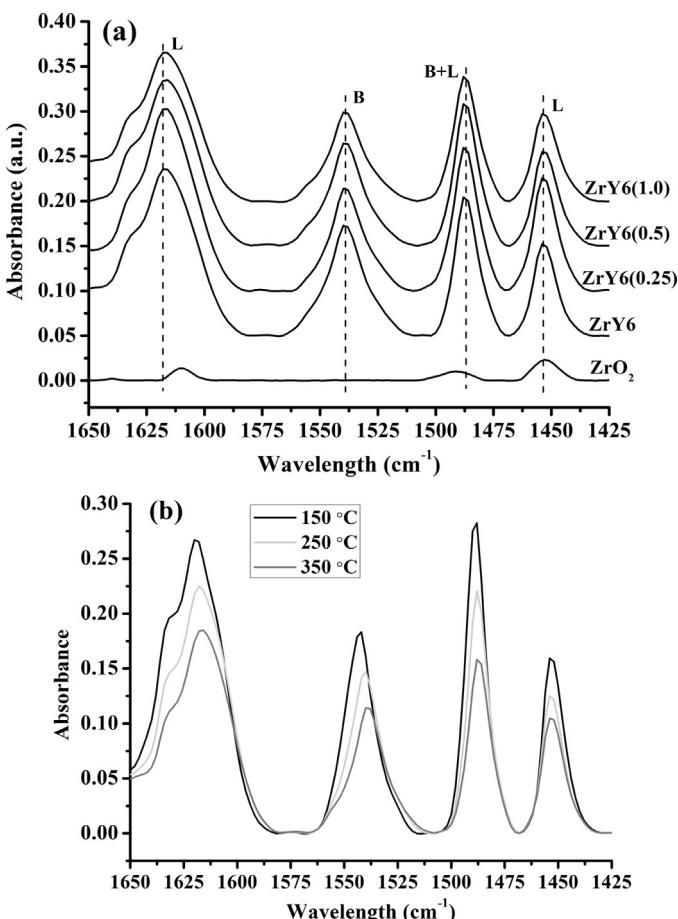


Fig. 5. Pyridine-adsorbed FT-IR spectra of (a) ZrO_2 , HY6 and ZrY6 hybrids at a desorption temperature of 350 °C, and (b) ZrY6(0.5) at different desorption temperatures of 150, 250 and 350 °C (B: Bronsted acid site, L: Lewis acid site).

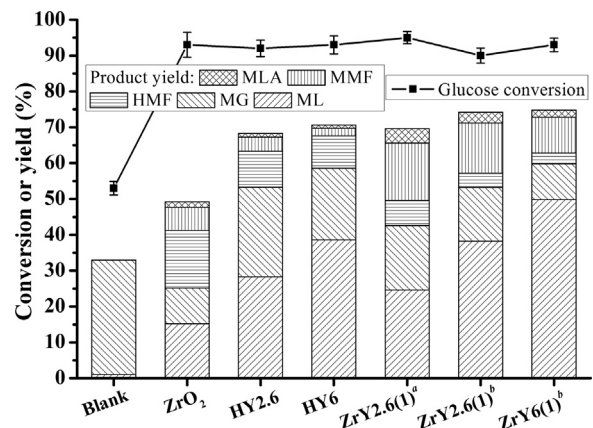


Fig. 6. Catalytic conversion of glucose to ML with different catalysts (Reaction conditions: 180 °C for 60 min, 10 g/L glucose, 30 mg catalyst and 5 mL methanol; Blank: without any catalyst). ^aPrepared by impregnation (IP) method; ^bprepared by deposition-precipitation (DP) method. (MMF: 5-methoxymethylfurfural, MLA: methyl lactate, HMF: 5-hydroxymethylfurfural, MG: methyl glucoside, ML: methyl levulinate).

of ZrO_2 with medium-strong basicity (Fig. S5) could facilitate the formation of basic sites on the hybrids.

The distribution of Bronsted and Lewis acid sites in ZrO_2 , HY6 and ZrY6 hybrids was examined by pyridine-adsorbed FT-IR (Fig. 5). Typically, the bands at around 1537 cm^{-1} , and at 1452 and 1615 cm^{-1} indicate the presence of Bronsted and Lewis acid sites, respectively, while the band at 1487 cm^{-1} is assigned to the combination of pyridine on both Lewis and Bronsted acid sites [45]. From Fig. 5, it can be found that ZrO_2 is free of Bronsted acid sites, while HY6 has both Bronsted and Lewis acid sites at a desorption temperature of 350 °C. The introduction of ZrO_2 onto HY6 can promote the formation of extra Lewis acid sites, accompanying with slight consumption of Bronsted acid sites (Fig. 5a, Table S1). Its interesting to note that the Bronsted acid site content and strength of ZrY6(0.5) are comparable to that of HY6 (Table S1) despite it decreases slightly with the increase of the desorption temperature (Fig. 5b).

3.2. Catalyst screening

Initial catalytic experiments were conducted to investigate the catalytic activity of acidic zeolites and metal-zeolite hybrids for producing ML from glucose at 180 °C for 60 min, and the possibly involved reaction pathways are shown in Scheme S1. The blank experiment without any catalyst afforded a trace amount of ML (~1% yield, Fig. 6), while a moderate glucose conversion of 53% was detected with MG as a major product (32% yield). The presence of ZrO_2 could give an enhanced glucose conversion (93%), with a certain amount of MG (10%), fructose/MF (<1%), HMF (16%) and MMF (8%), but still a low ML yield (15%), indicating that the metal oxide with more base sites promotes isomerization of glucose to fructose but is inactive for subsequent dehydration, etherification and rehydration reactions (Scheme S1). Interestingly, ML yield increased significantly to 30–40% with the presence of acidic zeolites (Fig. S6), except HZSM-5 having medium pore channels that possibly hinder the access of bulky molecules. These results illustrated that microwave irradiation really facilitated glucose conversion but gave the intermediates or byproducts like HMF, MMF and MG as dominant products, proving methanol as reaction medium could effectively suppress the formation of humins by generating methylated intermediates [46], and a higher temperature seemed favourable for ML production. Among different types of zeolites, HY and H β zeolites were more active than HZSM-

5, because they had larger pore channels for the access of bulky molecules in glucose conversion to ML. The HY6 zeolite with appropriate density of Lewis and Bronsted acid sites in high strength (Table S1, Fig. S7) was likely to facilitate glucose-fructose isomerization and dehydration/rehydration reactions, respectively [30], thus giving a higher yield of ML (39%) than the others, despite HY2.6 possessed more weak acid site content than HY6 and HY30 (Fig. S8, Table S2). Likewise, dealumination of H β zeolite by calcination at 700 °C was demonstrated to enhance its Lewis acidity [47], producing ML in an improved yield of up to 38% (Fig. S6). Nevertheless, in both cases, more Lewis acid sites were prone to form soluble polymers and humins.

To further study the influence of Lewis acidity on product selectivity, four different metal species (i.e., Fe, Zn, Cu and Zr) were deposited onto HY2.6 zeolite by IP method. It was found that relatively lower ML yields (15–24%) along with much more MG, MMF, MLA and humins were obtained over these metal-zeolite hybrids (Fig. S9), compared to neat HY2.6 zeolite (Fig. 6). Lewis acidity was helpful for isomerizing glucose to fructose, but could concurrently promote retro-alcohol reactions and methanolysis of cellulose to MG, which greatly hindered the formation of ML [28]. On the other hand, the presence of metal oxide was able to enhance the absorption of microwave irradiation in the catalytic system [39]. However, the resulting higher local reaction temperatures were more prone to cause side-reactions assisted with Lewis acidic centers, thus giving ML in lower yields. In an alternative way, the possession of acid and base couple sites in a single solid catalyst appeared to be more attractive for conversion of glucose to ML, wherein the sugar isomerization was facilitated by base sites [44], and the subsequent dehydration, rehydration, and esterification could be sequentially catalyzed by acid centers. Along with the presence of acid sites, ZrY2.6(1) prepared by DP method possessed a higher base site density of 0.05 mmol/g than the IP-synthesized catalyst (<0.01 mmol/g; Table S2). The possible interaction between chloride and metal species of ZrY2.6(1)-IP was proposed to increase the acid site content but interfere the generation of base sites [48]. Gratifyingly, ZrY2.6(1) and ZrY6(1) prepared by DP method could enhance ML yields reaching 38% and 50%, respectively, at a comparable glucose conversion (Fig. 6). The pyridine-adsorbed FT-IR illustrated that the DP catalyst ZrY2.6(1) showed a lower content of Lewis acid sites than the counterpart by IP method (Fig. S10), which could possibly contribute to inhibit the occurrence of side reactions. In particular, ZrY6(1)-DP with moderate contents of Lewis and Bronsted acid sites (Fig. S10) was more helpful for producing ML from glucose. These results proved the significant effect of acidic support type, metal species and preparation method on ML yield.

3.3. Effect of reaction time, temperature and zirconia content

ZrY6(1) prepared by DP method was further applied to study the influence of reaction time and temperature on producing ML from glucose under microwave irradiation (Fig. 7a). After reacting at 140 °C for 60 min, around 72% glucose was converted to ML with a low yield of 6%, but giving a massive amount of MG (~50%), along with minor HMF and MMF (~2%). As the reaction duration was prolonged to 300 min, glucose conversion and ML yield increased to 98% and 28%, respectively. The moderate ML yield lower than expected was probably resulted from the formation of stable methylated intermediates that are unable to perform downstream reactions. At a higher temperature of 160 °C, an improved ML yield of 40% at glucose conversion of 89% was observed in 60 min. With the increase of reaction time from 60 to 300 min, the ML yield was gradually raised to 57% with almost complete conversions. These results showed the significant role of temperature and time in further transforming the methylated intermediates to ML. It was deduced that MG was formed in the early stage and

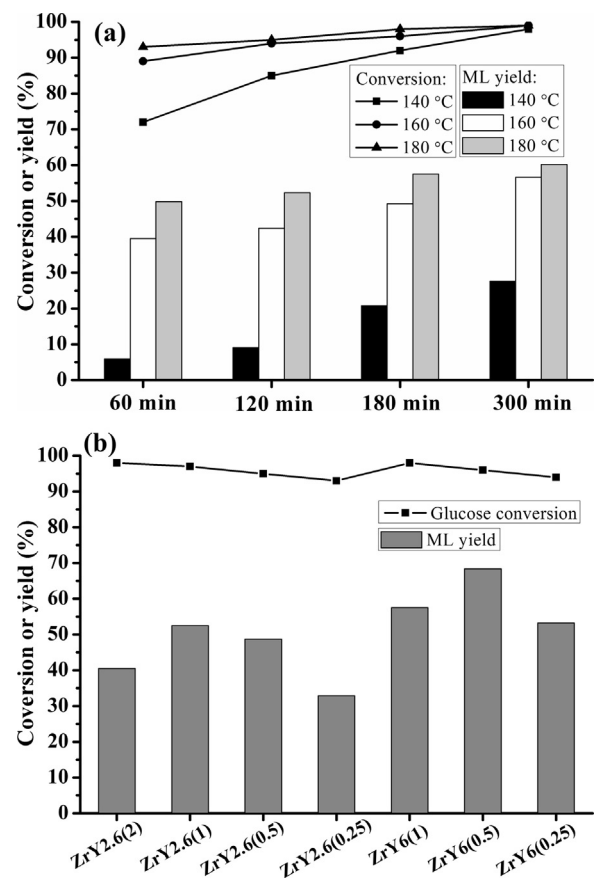


Fig. 7. Glucose conversion and ML yield varied with: (a) reaction time and temperature catalyzed by ZrY6(1)-DP hybrid (10 g/L glucose, 30 mg catalyst and 5 mL methanol), and (b) zirconia content deposited onto HY2.6 and HY6 zeolites using DP method (10 g/L glucose, 30 mg catalyst, 5 mL methanol, 180 °C and 180 min).

then gradually converted to MMF; in parallel, glucose was partially dehydrated to HMF in a short period of time followed by reacting with methanol to yield MMF. In a cross point, more time was probably required for the rehydration of MMF to ML. At a much higher temperature of 180 °C, 50–61% yields of ML were observed in the reaction duration of 60–300 min. Glucose and MMF were hardly observed by HPLC after 180 min, and the comparable ML yield in 180 and 300 min (58% vs. 61%) showed the completion of the reaction. However, soluble and black insoluble humins, which were found in small amounts during the reaction period of 60–180 min, were largely found after 300 min. Notably, fructose and MF were rarely detected at the temperature range of 140–180 °C, indicating the rapid conversion of these intermediates in the microwave reactor. Since reaction pressure reached about 2.6 MPa at 180 °C in the glass vial, which was very close to the limitation of 3.2 MPa (Fig. S1), a higher temperature (e.g., 200 °C) was not used for the reactions involving highly volatile methanol. Therefore, 180 °C and 180 min were selected as the optimal reaction conditions for next experiments.

As shown in Table 1, the content of ZrO₂ directly affected the density of acid and base sites in zirconia-Y6 hybrids. The influence of zirconium content on producing ML from glucose was thus evaluated at 180 °C for 180 min (Fig. 7b). ZrY6(1) with the highest zirconium content (1.0 mmol/g) exhibited a superior glucose conversion (98%), but gave a moderate ML yield (58%) that was lower than ZrY6(0.5) (68%) and comparable to ZrY6(0.25) (53%). It could be deduced from the results in Table 1 and Fig. 7b that the high local temperature around the Zr-O species caused by absorbing

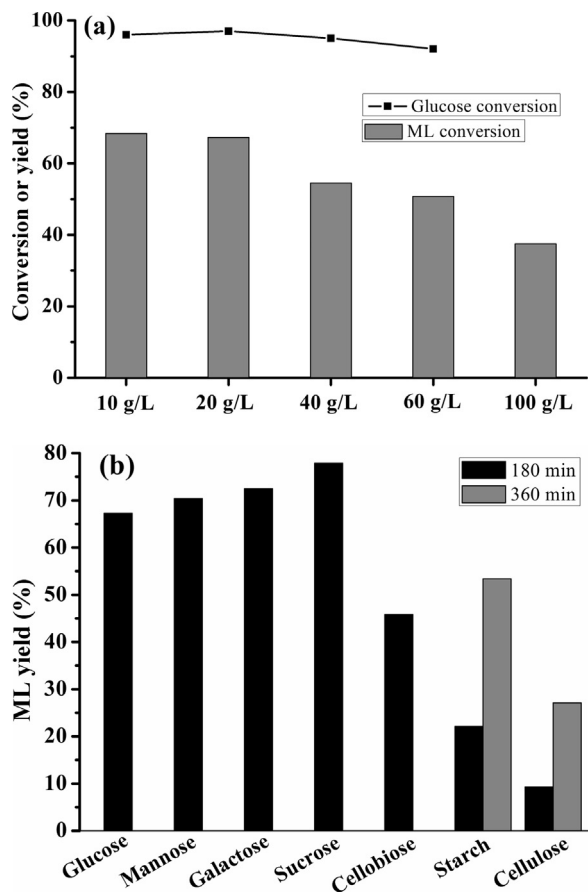


Fig. 8. Sugar conversion and ML yield varied with: (a) glucose concentration (30 mg ZrY6(0.5), 5 mL methanol, 180 °C and 180 min), and (b) different substrates (20 g/L substrate, 30 mg ZrY6(0.5), 5 mL methanol and 180 °C).

additional microwave energy was more likely to accelerate glucose conversion, compared to the high acid site content supplied by the zeolitic support. On the other hand, the appropriate balance between acid-base site density and local temperature in the case of ZrY6(0.5) seemed to produce ML with an enhanced yield. To check the universality of this finding, ZrY2.6 hybrids with different zirconium contents (0.25–2.0 mmol/g) were also utilized to catalyze glucose being converted to ML. In line with the results obtained over ZrY6 hybrids, the conversion of glucose (93–98%) was positively correlated with zirconium content of ZrY2.6 catalysts (Fig. 7b), while ML yield (33–53%) was associated with the quantity of both zirconium and acid-base sites (Table S2, Fig. S11). The ZrY6(0.5) hybrid with high ML yield (68%) and glucose conversion (96%) at 180 °C for 180 min was thus chosen as the catalyst for subsequent experiments.

3.4. Effect of glucose concentration and substrate

Different glucose concentrations (10–60 g/L) were used to further evaluate the catalytic performance of ZrY6(0.5) at 180 °C for 180 min. As illustrated in Fig. 8a, when glucose increased from 10 to 20 g/L, negligible fluctuations in ML yield (from 68% to 67%) and glucose conversion (from 96% to 97%) were observed. However, lower ML yields of 55% and 51% were obtained at high glucose concentrations of 40 and 60 g/L, respectively, despite glucose conversions were little changed. Interestingly, around 38% ML yield could still be achieved even though a large amount of glucose was insoluble into methanol at a high glucose concentration of 100 g/L (glucose con-

version not provided). Therefore, the optimal substrate conversion was set as 20 g/L in the following experimental runs.

Besides glucose, other biomass-derived mono-, di-, and polysaccharides including mannose, galactose, sucrose, cellobiose, starch, and cellulose were also tested under above optimal conditions. Fig. 8b demonstrated that high ML yields of ~70 and 73% could be obtained from mannose and galactose, respectively, showing the high activity of ZrY6(0.5) in selective conversion of different monosaccharides. Notably, a much higher ML yield of 78% was achieved from sucrose, and the presence of fructose units possibly contributed to the enhanced reactivity. In contrast, a moderate ML yield of 46% was attained from cellobiose (67% from glucose) because harsh reaction conditions such as additional acidity and longer time were required for the initial step of methanolysis. When using starch and cellulose as substrates, relatively lower ML yields of (9–22%) were achieved at 180 °C in 180 min. By prolonging reaction time from 180 to 360 min, improved ML yields of 53 and 27% could be realized from starch and cellulose, respectively. As a result, the microwave-assisted catalytic system over ZrY6(0.5) hybrid was suitable for transforming different types of biomass-derived sugars into ML under optimal reaction conditions.

3.5. Comparison with previous results

Different reported acidic systems under separately optimal reaction conditions were compared to this work for catalytic conversion of sugars to ML. In Table 2, the homogeneous mixed acids Al₂(SO₄)₃–H₂SO₄ containing Lewis–Bronsted acid sites were active for production of ML (54% yield) from glucose (100% conversion) [49]. However, the strong acid H₂SO₄ at a high temperature of 200 °C was employed, which was potentially corrosive to metal reactors. When a solid acid such as SBA-15 supported sulfated zirconia and commercial zeolite was employed, a considerable long reaction duration (20 or 24 h) at a moderate temperature (140 or 160 °C) was necessary to achieve high ML yields (25–49%) from glucose and restrain the formation of humins [26,30]. In this work, ZrY6(1) hybrid was able to produce ML with a comparable yield (50%) at 180 °C in 1 h. TiO₂ nanoparticles could also catalyze glucose being converted to ML with 61% yield at 175 °C, but a long reaction time (i.e., 9 h) was required [29]. The as-prepared ZrY6(0.5) catalyst remarkably improved the reaction processes (Table 2, entries 6 & 7) in terms of reaction duration (1–3 h), ML yield (up to 78%), and sugar conversion (93–99%) under microwave irradiation.

When the reactions were conducted with ZrY6(0.5) under identical conditions using a conventional heating mode (Table 2, entries 8 & 9), moderate yields of ML (32–46%) were obtained at almost complete glucose conversion after reacting for 3–9 h. It was interesting to note that a much shorter reaction duration was required for ZrY6(0.5) than the commercial zeolite HY6 (9 vs. 20 h) to acquire the comparative ML yields under conventional heating (Table 2, entry 9 vs. 3), despite ZrY6(0.5) showed the best catalytic performance under microwave irradiation. These results evidently indicated the promoting effect of microwave irradiation and Zr–O species deposited into the HY6 zeolite on conversion of sugars to ML, which most likely contributed to minimize the time on stream, thereby reducing humin formation and improving selectivity towards the product via the acid-base catalysis.

3.6. Proposed reaction mechanism

By local desilication with ammonia, nest silanols are formed from the framework of zeolites after calcination, which can not only be used as a base for grafting functional groups (e.g., metal oxides) [50–52], but also increase the pore diameters that can facilitate the access of bulky substrates (Table 1). The resulting acid-base pairs in the Si–O–M framework can well maintain the

Table 2

Comparison of different catalysts for producing ML from biomass-derived sugars.

Entry	Catalyst	Substrate	Temperature	Time	Conversion	ML yield	Ref.
1	$\text{Al}_2(\text{SO}_4)_3/\text{H}_2\text{SO}_4$	Glucose	200 °C	2 h	100%	54%	[43]
2	Grafted SZ/SBA-15	Glucose	140 °C	24 h	–	25%	[22]
3	H-USY(6)	Glucose	160 °C	20 h	–	49%	[26]
4	TiO ₂ nanoparticles	Glucose	175 °C	9 h	>99%	61%	[25]
5	ZrY6(1)	Glucose	180 °C	60 min	93%	50%	This work
6	ZrY6(0.5)	Glucose	180 °C	3 h	97%	67%	This work
7	ZrY6(0.5)	Sucrose	180 °C	3 h	99%	78%	This work
8 ^a	ZrY6(0.5)	Glucose	180 °C	3 h	95%	32%	This work
9 ^a	ZrY6(0.5)	Glucose	180 °C	9 h	>99%	46%	This work

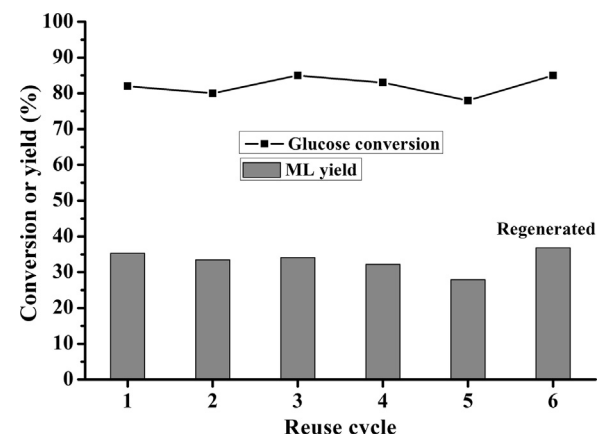
^a Reaction conducted in an autoclave reactor using a conventional heating mode excluding a heating time of 0.5 h to 180 °C.

activity of Lewis acid and base sites, unlike traditional acid in basic solutions [53]. In the process of glucose-to-ML conversion over ZrY6(0.5), sugar isomerization promoted by Lewis acid and base sites, and saccharide ring-open to linear chain (1,2-enediol) by Bronsted and Lewis acid sites both occur on the surface of the hybrid. However, MG will be significantly generated in the presence of excess Bronsted acid sites. The linear 1,2-enediol is more prone to diffuse into the catalyst pores, wherein HMF and MMF can be formed over Bronsted and/or Lewis acid sites through dehydration and dehydration-etherification, respectively. The resulting intermediates HMF and MMF with furan-ring are most likely to be trapped in the micropores of zeolites, which can be further rehydrated (rehydrated-esterified) to produce ML and MFM catalyzed by inner Bronsted acid sites. In parallel, the presence of surplus Lewis acid/base sites may incur side reactions (e.g., retro-Aldol) to give byproducts like MLA under relatively harsh conditions. Therefore, the pore size, acid-base sites distribution, and shape selectivity of the modified zeolites, as well as reaction conditions directly affect the catalytic transformation of sugars to ML.

3.7. Catalyst recycling study

Before carrying out catalyst recycling study, the ZrY6(0.5) catalyst dosage was optimized to evaluate the reactivity of the used catalytic systems (Fig. S12). Under the optimized reaction conditions, no obvious decrease in glucose conversion (97–82%) while a significant loss of ML yields (67–35%) were observed when the catalyst amount was reduced from 30 to 10 mg, indicating the necessity of enough acid-base sites to achieve high ML yields. However, further increasing the catalyst dosage to 40 or 50 mg did not lead to a distinct increase in ML yield, owing to the formation of stable methylated products and humins [46].

Initially, ZrY6(0.5) with the optimal catalyst dosage (30 mg) was used for the recycling study at 180 °C for 180 min (Fig. S13). In five consecutive cycles, glucose conversion maintained >95% with stable ML yields (63–67%). At a much lower catalyst dosage of 10 mg, the reusability of ZrY6(0.5) was also investigated under identical reaction conditions (Fig. 9). Almost constant glucose conversion (80–85%) and ML yield (32–35%) were observed from the first to fourth cycle. Although the performance of ZrY6(0.5) slightly decreased in the fifth cycle (with 78% conversion and 28% ML yield), the regenerated ZrY6(0.5) by calcination at 450 °C for 4 h could produce ML with a comparable yield to the fresh catalyst. TG analysis showed that around 8 wt% organic matter was adsorbed in ZrY6(0.5) after five cycles (Fig. 10a), and the regeneration process could remove partial organic residues to activate the catalyst (Figs. 9 and 10 a). XRD pattern and IR spectrum of the recovered ZrY6(0.5) after five cycles were well consistent with those of the fresh one (Fig. 10b and c), revealing the durable structure of the catalyst in methanol at 180 °C. The slightly reduced intensity in both XRD and IR spectra also demonstrated the adsorption of organic

**Fig. 9.** Recyclability of ZrY6(0.5) catalyst in glucose-to-ML conversion ($T = 180^\circ\text{C}$, $t = 180\text{ min}$, 20 g/L glucose, 10 mg catalyst and 5 mL methanol).

molecules onto the surface of the catalyst during reactions. Moreover, NH_3 -TPD profiles showed a trivial decrease in acidity from 0.97 to 0.84 mmol/g after five cycles (Fig. 10d), which was possible due to the coverage of the catalyst surface by humins (BET surface area decreasing from 655.7 to 598.9 $\text{m}^2\text{ g}^{-1}$). The leaching of partial zirconia into methanol (<1 ppm) was likely to cause the slight decline of base site content of ZrY6(0.5) from 0.08 to 0.06 mmol/g in five consecutive cycles (Fig. S14). About 7% zirconium and 3% aluminium species of the ZrY6(0.5) hybrid recovered in the fifth run were lost, indicating that metal leaching occurred to relatively small extents during the catalytic reaction.

4. Conclusions

Acid-base bifunctional zirconia-zeolite hybrid ZrY6(0.5) with high stability and porosity was prepared, and demonstrated to show superior activity to previously reported acidic systems in direct production of ML from carbohydrates. In the presence of ZrY6(0.5), high ML yields (up to 73%) could be achieved from monosaccharides (glucose, mannose and galactose) at 180 °C for 180 min. Particularly, an even higher ML yield of 78% was obtained from sucrose. For polysaccharides, moderate ML yields of 53 and 27% were able to be produced from starch and cellulose, respectively. The acid-base bifunctionality and zirconia-enhanced microwave absorption were possibly contributed to the high performance of ZrY6(0.5) in producing ML. Moreover, the catalyst could be reused for at least five times with stable conversion rates and ML yields.

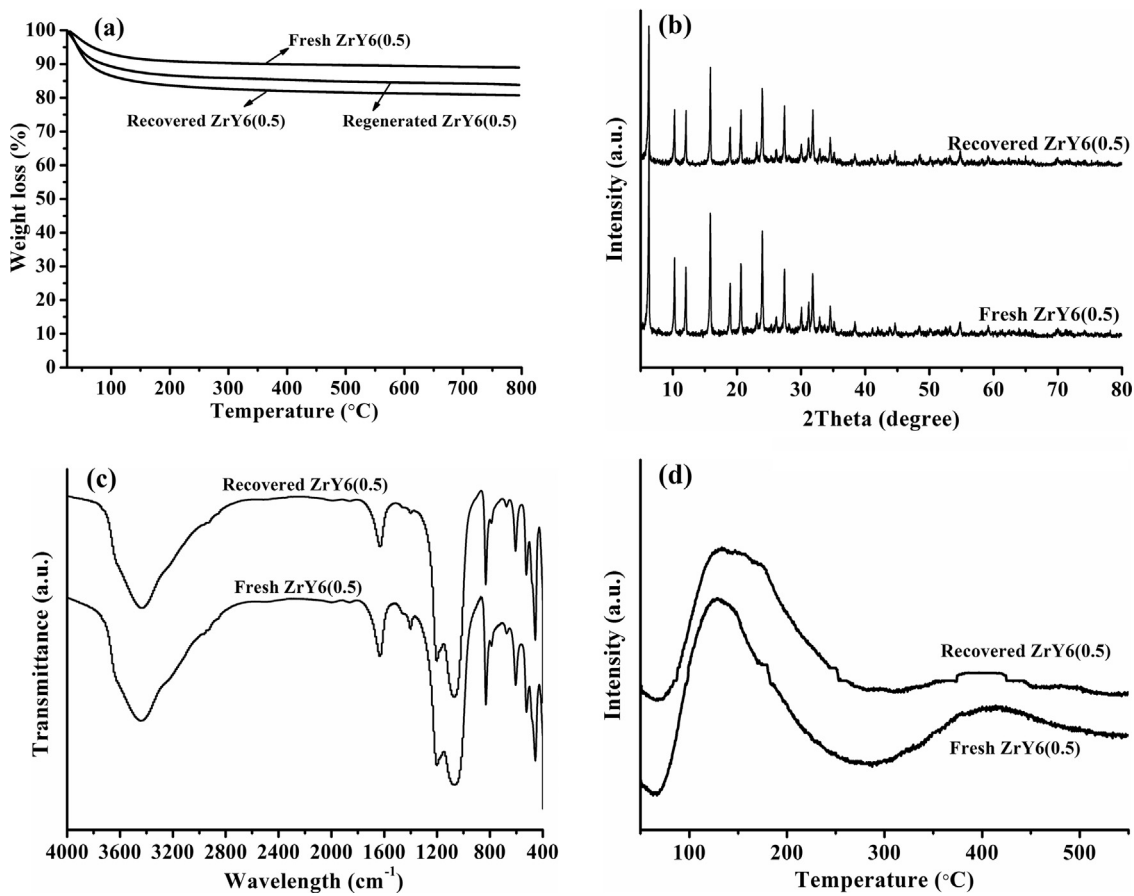


Fig. 10. (a) TG curves, (b) XRD patterns, (c) FT-IR spectra, and (d) NH_3 -TPD profiles of fresh and recovered (after five cycles) $\text{ZrY6}(0.5)$ catalysts.

Acknowledgements

This work is financially supported by the Nanjing Agricultural University (68Q-0603), Chinese Academy of Sciences [Equipment R&D grant (YZ201260) & 135 program (XTBG-T02)], National Natural Science Foundation of China (21576059), and Yunnan Provincial Government (Hundreds of High-Level Overseas Talents).

Appendix A. Supplementary data

Supplementary data associated with this article can be found, in the online version, at <http://dx.doi.org/10.1016/j.apcatb.2016.07.007>.

References

- [1] J.C. Serrano-Ruiz, J.A. Dumesic, Catalytic routes for the conversion of biomass into liquid hydrocarbon transportation fuels, *Energy Environ. Sci.* 4 (2011) 83–99.
- [2] H. Li, Z. Fang, R.L. Smith Jr., S. Yang, Efficient valorization of biomass to biofuels with bifunctional solid catalytic materials, *Prog. Energy Combust.* 55 (2016) 98–194.
- [3] J.J. Bozell, G.R. Petersen, Technology development for the production of biobased products from biorefinery carbohydrates—the US Department of Energy's top 10 revisited, *Green Chem.* 12 (2010) 539–554.
- [4] D.W. Rackemann, W.O. Doherty, The conversion of lignocellulosics to levulinic acid, *Biofuel Bioprod.* 5 (2011) 198–214.
- [5] P. Sun, G. Gao, Z. Zhao, C. Xia, F. Li, Acidity-regulation for enhancing the stability of Ni/HZSM-5 catalyst for valeric biofuel production, *Appl. Catal. B: Environ.* 189 (2016) 19–25.
- [6] K. Yan, Y. Yang, J. Chai, Y. Lu, Catalytic reactions of gamma-valerolactone: a platform to fuels and value-added chemicals, *Appl. Catal. B: Environ.* 179 (2015) 292–304.
- [7] S.G. Wettstein, J.Q. Bond, D.M. Alonso, H.N. Pham, A.K. Datye, J.A. Dumesic, RuSn bimetallic catalysts for selective hydrogenation of levulinic acid to γ -valerolactone, *Appl. Catal. B: Environ.* 117–118 (2012) 321–329.
- [8] A. Morone, M. Apte, R.A. Pandey, Levulinic acid production from renewable waste resources: bottlenecks, potential remedies, advancements and applications, *Renewable Sustainable Energy Rev.* 51 (2015) 548–565.
- [9] H. Kobayashi, H. Ohta, A. Fukuoka, Conversion of lignocellulose into renewable chemicals by heterogeneous catalysis, *Catal. Sci. Technol.* 2 (2012) 869–883.
- [10] H. Li, Q. Zhang, S.P. Bhadury, S. Yang, Furan-type compounds from carbohydrates via heterogeneous catalysis, *Curr. Org. Chem.* 18 (2014) 547–597.
- [11] P. Carniti, A. Gervasini, F. Bossola, V.D. Santo, Cooperative action of Brønsted and Lewis acid sites of niobium phosphate catalysts for cellobiose conversion in water, *Appl. Catal. B: Environ.* 193 (2016) 93–102.
- [12] X. Tang, H. Chen, L. Hu, W. Hao, Y. Sun, X. Zeng, L. Lin, S. Liu, Conversion of biomass to γ -valerolactone by catalytic transfer hydrogenation of ethyl levulinate over metal hydroxides, *Appl. Catal. B: Environ.* 147 (2014) 827–834.
- [13] A. Mukherjee, M.J. Dumont, V. Raghavan, Review: sustainable production of hydroxymethylfurfural and levulinic acid: challenges and opportunities, *Biomass Bioenergy* 72 (2015) 143–183.
- [14] Y. Zuo, Y. Zhang, Y. Fu, Catalytic conversion of cellulose into levulinic acid by a sulfonated chloromethyl polystyrene solid acid catalyst, *ChemCatChem* 6 (2014) 753–757.
- [15] P.P. Upare, J.W. Yoon, M.Y. Kim, H.Y. Kang, D.W. Hwang, Y.K. Hwang, H.H. Kung, J.S. Chang, Chemical conversion of biomass-derived hexose sugars to levulinic acid over sulfonic acid-functionalized graphene oxide catalysts, *Green Chem.* 15 (2013) 2935–2943.
- [16] J. Zhang, S. Wu, H. Zhang, B. Li, Conversion of glucose over $\text{SO}_4^{2-}/\text{ZrO}_2\text{-TiO}_2$ catalysts in an extremely low acid system, *Bioresources* 7 (2012) 3984–3998.
- [17] R. Weingarten, Y.T. Kim, G.A. Tompsett, A. Fernandez, K.S. Han, E.W. Hagaman, W.C. Conner, J.A. Dumesic, G.W. Huber, Conversion of glucose into levulinic acid with solid metal (IV) phosphate catalysts, *J. Catal.* 304 (2013) 123–134.
- [18] X. Hu, S. Kadarwati, S. Wang, Y. Song, M.D.M. Hasan, C.Z. Li, Biomass-derived sugars and furans: which polymerize more during their hydrolysis? *Fuel Process. Technol.* 137 (2015) 212–219.
- [19] R. Weingarten, W.C. Conner, G.W. Huber, Production of levulinic acid from cellulose by hydrothermal decomposition combined with aqueous phase dehydration with a solid acid catalyst, *Energy Environ. Sci.* 5 (2012) 7559–7574.

- [20] S.G. Wettstein, D.M. Alonso, Y. Chong, J.A. Dumesic, Production of levulinic acid and gamma-valerolactone (GVL) from cellulose using GVL as a solvent in biphasic systems, *Energy Environ. Sci.* 5 (2012) 8199–8203.
- [21] S. Tabasso, E. Montoneri, D. Carnaroglio, M. Capraso, G. Cravotto, Microwave-assisted flash conversion of non-edible polysaccharides and post-harvest tomato plant waste to levulinic acid, *Green Chem.* 16 (2014) 73–76.
- [22] K.W. Omari, J.E. Besaw, F.M. Kerton, Hydrolysis of chitosan to yield levulinic acid and 5-hydroxymethylfurfural in water under microwave irradiation, *Green Chem.* 14 (2012) 1480–1487.
- [23] H. Ren, Y. Zhou, L. Liu, Selective conversion of cellulose to levulinic acid via microwave-assisted synthesis in ionic liquids, *Bioresour. Technol.* 129 (2013) 616–619.
- [24] Á. Szabolcs, M. Molnár, G. Dibó, L.T. Mika, Microwave-assisted conversion of carbohydrates to levulinic acid: an essential step in biomass conversion, *Green Chem.* 15 (2013) 439–445.
- [25] S. Hassanzadeh, N. Aminlashgari, M. Hakkarainen, Chemo-selective high yield microwave assisted reaction turns cellulose to green chemicals, *Carbohydr. Polym.* 112 (2012) 448–457.
- [26] G. Morales, A. Osatiashvili, B. Hernández, J. Iglesias, J.A. Melero, M. Paniagua, D.R. Brown, M. Granollers, A.F. Lee, K. Wilson, Conformal sulfated zirconia monolayer catalysts for the one-pot synthesis of ethyl levulinate from glucose, *Chem. Commun.* 50 (2014) 11742–11745.
- [27] A. Deimolis, N. Essayem, F. Rataboul, Synthesis and applications of alkyl levulimates, *ACS Sustainable Chem. Eng.* 2 (2014) 1338–1352.
- [28] D. Ding, J. Xi, J. Wang, X. Liu, G. Lu, Y. Wang, Production of methyl levulinate from cellulose: selectivity and mechanism study, *Green Chem.* 17 (2015) 4037–4044.
- [29] C.H. Kuo, A.S. Poyraz, L. Jin, Y. Meng, L. Pahalagedara, S.Y. Chen, D.A. Kriz, C. Guild, A. Gudz, S.L. Suib, Heterogeneous acidic TiO_2 nanoparticles for efficient conversion of biomass derived carbohydrates, *Green Chem.* 16 (2014) 785–791.
- [30] S. Saravanamurugan, A. Riisager, Zeolite catalyzed transformation of carbohydrates to alkyl levulimates, *ChemCatChem* 5 (2013) 1754–1757.
- [31] N. Ya'aini, N.A.S. Amin, S. Endud, Characterization and performance of hybrid catalysts for levulinic acid production from glucose, *Microporous Mesoporous Mater.* 171 (2013) 14–23.
- [32] S. Saravanamurugan, O. Nguyen van Buu, A. Riisager, Conversion of mono- and disaccharides to ethyl levulinate and ethyl pyranoside with sulfonic acid-functionalized ionic liquids, *ChemSusChem* 4 (2011) 723–726.
- [33] S. Saravanamurugan, A. Riisager, Solid acid catalysed formation of ethyl levulinate and ethyl glucopyranoside from mono-and disaccharides, *Catal. Commun.* 17 (2012) 71–75.
- [34] T.C. Su, Z. Fang, F. Zhang, J. Luo, X.K. Li, Hydrolysis of selected tropical plant wastes catalyzed by a magnetic carbonaceous acid with microwave, *Sci. Rep.* 5 (2015) 17538.
- [35] S.P. Fan, L.Q. Jiang, C.H. Chia, Z. Fang, S. Zakaria, K.L. Chee, High yield production of sugars from deproteinized palm kernel cake under microwave irradiation via dilute sulfuric acid hydrolysis, *Bioresour. Technol.* 153 (2014) 69–78.
- [36] F. Guo, Z. Fang, T.J. Zhou, Conversion of fructose and glucose into 5-hydroxymethylfurfural with lignin-derived carbonaceous catalyst under microwave irradiation in dimethyl sulfoxide–ionic liquid mixtures, *Bioresour. Technol.* 112 (2012) 313–318.
- [37] F. Mushtaq, R. Mat, F.N. Ani, A review on microwave assisted pyrolysis of coal and biomass for fuel production, *Renewable Sustainable Energy Rev.* 39 (2014) 555–574.
- [38] T. Ennaert, J.V. Aelst, J. Dijkmans, R.D. Clercq, W. Schutyser, M. Dusselier, D. Verboekend, B.F. Sels, Potential and challenges of zeolite chemistry in the catalytic conversion of biomass, *Chem. Soc. Rev.* 45 (2016) 584–611.
- [39] J. González-Rivera, I.R. Galindo-Esquivel, M. Onor, E. Bramanti, I. Longo, C. Ferrari, Heterogeneous catalytic reaction of microcrystalline cellulose in hydrothermal microwave-assisted decomposition: effect of modified zeolite Beta, *Green Chem.* 16 (2014) 1417–1425.
- [40] N.A.S. Ramli, N.A.S. Amin, Fe/HY zeolite as an effective catalyst for levulinic acid production from glucose: characterization and catalytic performance, *Appl. Catal. B: Environ.* 163 (2015) 487–498.
- [41] A. Osatiashvili, A. Lee, M. Granollers, D. Brown, L. Olivi, G. Morales, J. Melero, K. Wilson, Hydrothermally stable conformal, sulfated zirconia monolayer catalysts for glucose conversion to 5-HMF, *ACS Catal.* 5 (2015) 4345–4352.
- [42] K. Yan, T. Lafleur, J. Liao, Facile synthesis of palladium nanoparticles supported on multi-walled carbon nanotube for efficient hydrogenation of biomass-derived levulinic acid, *J. Nanopart. Res.* 15 (2013) 1906–1912.
- [43] Y. Tao, H. Kanoh, L. Abrams, K. Kaneko, Mesopore-modified zeolites: preparation, characterization, and applications, *Chem. Rev.* 106 (2006) 896–910.
- [44] X. Qi, M. Watanabe, T.M. Aida, R.L. Smith, Synergistic conversion of glucose into 5-hydroxymethylfurfural in ionic liquid–water mixtures, *Bioresour. Technol.* 109 (2012) 224–228.
- [45] M. Tao, L. Xue, Z. Sun, S. Wang, X. Wang, J. Shi, Tailoring the synergistic Brønsted–Lewis acidic effects in heteropolyacid catalysts: applied in esterification and transesterification reactions, *Sci. Rep.* 5 (2015) 13764.
- [46] X. Hu, C.Z. Li, Levulinic esters from the acid-catalysed reactions of sugars and alcohols as part of a biorefinery, *Green Chem.* 13 (2011) 1676–1679.
- [47] R. Otomo, T. Yokoi, J.N. Kondo, T. Tatsumi, Dealuminated Beta zeolite as effective bifunctional catalyst for direct transformation of glucose to 5-hydroxymethylfurfural, *Appl. Catal. A: Gen.* 470 (2014) 318–326.
- [48] C. Hammond, M.T. Schumperli, S. Conrad, I. Hermans, Hydrogen transfer processes mediated by supported iridium oxide nanoparticles, *ChemCatChem* 5 (2013) 2983–2990.
- [49] L. Peng, H. Li, L. Lin, K. Chen, Effect of metal salts existence during the acid-catalyzed conversion of glucose in methanol medium, *Catal. Commun.* 59 (2015) 10–13.
- [50] K. Na, M. Choi, R. Ryoo, Recent advances in the synthesis of hierarchically nanoporous zeolites, *Microporous Mesoporous Mater.* 166 (2013) 3–19.
- [51] T.C. Keller, S. Isabettini, D. Verboekend, E.G. Rodrigues, J. Pérez-Ramírez, Hierarchical high-silica zeolites as superior base catalysts, *Chem. Sci.* 5 (2014) 677–684.
- [52] T.C. Keller, K. Desai, S. Mitchell, J. Pérez-Ramírez, Design of base zeolite catalysts by alkali-metal grafting in alcoholic media, *ACS Catal.* 5 (2015) 5388–5396.
- [53] J.D. Lewis, S. Van de Vyver, Y. Román-Leshkov, Acid–base pairs in Lewis acidic zeolites promote direct Aldol reactions by soft enolization, *Angew. Chem. Int. Ed.* 54 (2015) 9835–9838.